Design, Simulation, and Optimisation of Sustainable Fertiliser Production: A Case Study of a Large-Scale Urea Facility in Italy

Safikri Aji Pratama[a], Shifa Gumuruh[a], Sultan Salman[a], Robith Hadhromi[a], Ihsaan Furlonge[a]

[a]*Department of Chemical Engineering, Imperial College London, London, SW7 2AZ, , United Kingdom*

Abstract

Nitrogen-based fertilisers are pivotal for global food security, yet their production is a notable source of greenhouse gas emissions. Urea, a vital fertiliser with significant market presence—19% in Europe and 33% globally—is produced through an energy-demanding process reliant on fossil fuels. This study introduces a 'Green' Urea plant concept, aimed for implementation in Ravenna, Italy, harnessing exclusively renewable energy sources to foster agricultural sustainability. With a production capacity of 1,300 tonnes per day, this facility neighbours Italy's first carbon capture and storage (CCS) facility at Ravenna. The core of the proposed methodology is the synthesis of green ammonia. Seawater Reverse Osmosis-Polymer Electrolyte Membrane Electrolysis (SWRO-PEM) and Pressure Swing Adsorption (PSA) yield the necessary hydrogen and nitrogen feedstocks. An enhanced Haber-Bosch process utilising a Ru-based catalyst, facilitating lower operational conditions (500°C and 100 bar) for the aforementioned reagents. Urea synthesis integrates CO_2 captured both from the adjacent Ravenna CCS and Direct Air Capture (DAC) systems, culminating in a closed-loop operation. Simulation of the PSA, Haber-Bosch, and Urea processes is conducted via Aspen Hysys, complemented by a GUROBI Python-based linear cost minimisation model to calculate the optimal mix of wind and solar energy, ensuring year-round production congruent with real-world climate patterns. Energy storage and discharge is modelled to minimise excess energy loss. Moreover, utility costs are optimised through Heat Exchanger Network integration and a cost minimisation model implemented in GAMS Studio. An environmental assessment, using OpenLCA, contrasts the 'Green' plant's footprint with traditional urea manufacturing, examining economic, environmental, and thermodynamic Key Performance Indicators (KPIs). The integrated modelling and KPI analysis provide evidence to suggest that the proposed plant's fiscal viability, environmental footprint, and N_2 conversion present a viable competitor to conventional synthesis, illustrating the plant's potential as a substantial leap toward greener fertiliser production.

Keywords: Renewable Electricity, Green Urea, Renewable Energy Optimisation, Direct Air Capture, CO_2

1. Introduction

According to the latest data for the 3^{rd} quarter of 2023 from the European Union (EU), 787 million tons of CO_2 equivalent (CO_{2-eq}) were released [1] [2]. The most contributing sectors are manufacturing (23.5%), households (17.9%), electricity, gas supply (15.5%), agriculture (14.3%), followed by transportation and storage (12.8%), all of which are above the Organisation for Economic Co-operation and Development (OECD) of 10%. Specifically (2022) Italy released 333.10 million tons of CO_2 [3], and on 2023 has successfully reduced its emissions by 5% while maintaining its Gross Domestic Product (GDP) [4]. Forecasts suggest that the agricultural industry in Italy is set to grow from USD 26.86bn in 2024 to USD 29.06bn in 2028 (Compound Annual Growth Rate of 1.99%, with an annual growth rate of the export market of 4.69%). As such, in the interest of bolstering the economy and remediating greenhouse gas emission of Italy and the EU at large, significant effort must be made to transition large-scale agrochemical processes to sustainable technologies.

The chosen region, Italy, is a promising candidate as a model nation in the global effort to abate greenhouse gas emissions and leverage emerging renewable energy technologies in the pursuit of environmentally sustainable chemical industries. In particular, Italy is poised and constantly progressing to its lofty goals, one of which is for 65% of its electricity from renewables by 2030, already boasting a third of electricity hailing from renewable sources. Furthermore, according to Italy's Eighth National Communication (NC8) and Fifth Biennial Report (BR5) on its adherence to the Paris Agreement [4]:

- *Emission Trends*: Italy's emissions have shown a notable decrease, attributed to economic restructuring, technological advancements, and policy interventions. The energy sector, including industrial processes, has seen significant shifts towards renewable sources and energy efficiency improvements. Italy's commitments under the EU's collective targets are underscored, with specific national targets set for sectors outside the EU Emission Trading Scheme (ETS). The NRRP is instrumental in aligning national efforts with broader EU objectives for 2030 and beyond, emphasising ecological transition and sustainability.

- *Scenario Analysis*: Projections under With Existing Measures (WEM) and With Additional Measures (WAM) scenarios indicate a downward trend in emissions, reflecting

the expected impact of current and planned policies. The scenarios suggest that Italy is on track to meet its 2030 and 2040 targets, with the energy sector anticipated to contribute the most significant emission reductions.

- *Sensitivity Analyses*: Sensitivity analyses on GDP growth and the price of CO_2 emission allowances highlight the robustness of Italy's projections and the potential impacts of economic and policy variables on emission trends.

Given the aforementioned policies and long-term plans for emissions reduction in Italy, this project aims to partake in and bolster these efforts. In particular it is proposed that utilising CO_2 as a feedstock in renewably powered processes for the production of high value chemicals such as methanol, olefins and urea sets up a two-hit protocol whereby CO_2 levels are abated while high value, in-demand chemicals are generated.

In 2021, Italy consumed approximately 572,100 tons of nitrogen fertilisers, representing 6% of total European consumption [4]. Urea, a major nitrogen-based fertiliser, emerges as a high-value candidate for sustainable production methodologies, especially when utilising CO_2 as a feedstock. Furthermore, the development of such a process contributes significantly to the sustainable development goals (SDGs), particularly SDG 7 (Affordable and Clean Energy), SDG 12 (Responsible Consumption and Production), and SDG 13 (Climate Action). The shift towards renewable energy in chemical manufacturing not only decarbonises industrial processes but also fosters innovation in green chemistry and circular economy practices.

This report aims to offer an economically, financially, and environmentally feasible large-scale, renewably powered urea production plant; a proposition which will enhance Italy's adherence to the Paris Agreement and the UN Sustainability Goals. The report is structured as follows: In Section 2, the value proposition of the sustainable production of Urea is discussed. This is followed by an assessment of the considered technologies relevant to urea production and the relevant performance indicators which informed the chosen processes. Section 3 discusses the processes for the derivation of the renewable feedstocks (H_2, N_2, CO_2) and the framework of integrated renewable electricity generation. The chosen pathways for ammonia and urea synthesis are explained in Section 5. Section 6 presents the simulations and models of all of the chosen processes. The Heat Exchanger Network (HEN) integration, utility cost minimisation and renewable energy optimisation is presented and explained in Section 7. Section 8 outlines the economic analysis which was conducted. Section 9 analyses the environmental impact of the proposed plant.

2. Urea as The Key Chemical

The selection of urea as the chemical of choice for a novel process design utilising captured CO_2 and renewable energy sources is underpinned by several compelling factors that align with the objectives of sustainable development and emissions reduction. Urea ($CO(NH_2)_2$) stands as one of the most extensively used nitrogenous fertilisers globally, owing to its high nitrogen content (approximately 46%), cost-effectiveness, and versatility in its application methods. Its widespread prevalence in agricultural practices is a testament to its efficacy in enhancing soil fertility and promoting crop yield, thus playing a pivotal role in global food security.

However, the traditional synthesis of urea is markedly carbon and energy-intensive, primarily involving the ammonia and CO_2 reaction under high temperature and pressure conditions. This process, predominantly reliant on fossil fuels for both feedstock (natural gas as the hydrogen source for ammonia production) and energy, significantly contributes to greenhouse gas (GHG) emissions. The Haber-Bosch process for ammonia synthesis, a precursor to urea production, is alone responsible for about 1-2% of global CO_2 emissions, underscoring the urgent need to rethink and redesign the urea production pathway [5].

2.1. Market Analysis

Valued at USD 57.2bn in 2021, the global market for nitrogenous fertilisers is expected to grow at a CAGR of 5.7% from 2022 to 2030, cementing it as the backbone of the agricultural industry. This expansion is a result of the burgeoning commercial agriculture sector worldwide. The agricultural industry's demand for nitrogenous fertilisers, due to their role in delivering essential nutrients and enhancing food crop yields, is a significant growth driver. These fertilisers are particularly pivotal in cultivating various agricultural commodities such as vegetables, fruits, cotton, and cereals.

Furthermore, as of 2021, urea accounts for the highest market share at 33%. As such, it is considered the most crucial nitrogenous fertiliser, rendering a promising, high-potential chemical in the context of large-scale sustainable transition given that it also necessitates CO_2 as a feedstock.

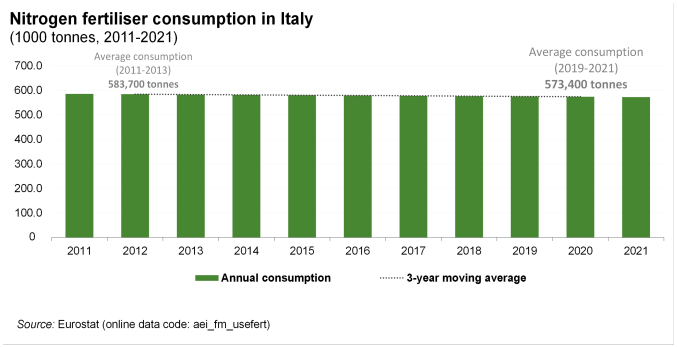

Figure 1: Urea consumption in Italy between 2011-2021

Figure 1 presents the demand for urea in Italy, displaying stability over a decade. From 2011 to 2021, there was a decrease in consumption. The early average (2011-2013) was 583,700 tonnes, and the more recent period (2019-2021) averages at 573,400 tonnes, indicating a slight downward trend in urea use.

The proposition to utilise captured CO_2 as a feedstock for urea production presents a twofold advantage: it aids in mitigating CO_2 emissions by sequestering carbon into a valuable product and diminishes the dependency on fossil-based resources. Moreover, integrating renewable energy into this process design

addresses the challenge of the energy transition in the chemical sector. By leveraging renewable energy sources to power the synthesis process, we can substantially reduce the carbon footprint of urea production, aligning it with the goals of the Paris Agreement and broader sustainability objectives.

In conclusion, the choice of urea as a target chemical for production using captured CO_2 and renewable energy is justified by its critical role in agriculture, the environmental impact of its conventional production methods, and the potential for significant sustainability gains through process redesign. This approach not only exemplifies the integration of renewable energy sources in chemical manufacturing but also proposes a forward-looking strategy to reduce industrial carbon emissions and reliance on fossil resources. As such, focusing on urea embodies a holistic, innovative response to the challenges faced by the chemical industry in the context of the energy transition and climate change mitigation.

2.2. State of the Art

2.2.1. Conventional Urea Production

The typical urea production process usually utilises natural gas to be converted into ammonia and CO_2. The plant consists of a reforming unit, CO_2 separation unit, methanation unit, cryogenic distillation column, ammonia synthesis unit, and the urea synthesis unit. In the initial step of the reforming process within the primary reformer unit, methane reacts with steam under a specific pressure ranging from 3-25 bar with the aid of a nickel catalyst to produce hydrogen, carbon monoxide, and a minor amount of CO_2. This reaction requires external heat due to its endothermic nature. Notably, the steam flow rate is not sufficient for complete conversion of the methane present in the feed stream. In the subsequent secondary reformer stage, a controlled amount of ambient air is introduced to provide the necessary oxygen for partial oxidation of the remaining natural gas, thereby introducing nitrogen into the main stream. The proportions of air and steam need to be carefully adjusted to ensure complete conversion of the fuel and to yield the required hydrogen-to-nitrogen (H_2:N_2) molar ratio of 3:1 for the subsequent ammonia synthesis process.

The final step in the reforming unit involves the shift reaction, where carbon monoxide reacts with steam in the presence of an iron catalyst to produce CO_2 and hydrogen. The process gas then undergoes CO_2 separation using absorption techniques employing amine solvents. Although most of the CO_2 is removed in this unit, a residual amount typically remains due to the unit's inefficiency. As even trace amounts of carbon monoxide and CO_2 act as catalyst poisons in ammonia synthesis, a further carbon monoxide removal unit is employed to ensure complete elimination. Various methods such as cryogenic distillation, Temperature Swing Adsorption (TSA) with COSORB solution, membrane technology, and Pressure Swing Adsorption (PSA) are utilised for carbon monoxide removal. The gas stream is then compressed and directed over a catalyst where nitrogen and hydrogen combine to form ammonia. Finally, the separated CO_2 and synthetic ammonia are processed further to yield urea as the end product [6].

As for the urea synthesis, the most widely used method globally is the stamicarbon process which involves two steps. The first one is the ammonium carbamate formation which is produced from the heterogeneous reaction of ammonia and CO_2 at approximately 150-250 bar and $180 - 190°C$. Then, the liquid product will be dehydrated to form urea at high pressure [7].

2.2.2. Sustainable Urea Production

The biggest challenges in urea production are its energy-intensiveness and low single-pass conversion. A novel urea synthesis technology offers several advancements over traditional urea synthesis processes. This energy-efficient method primarily reduces plant construction and operating costs and also enhances CO_2 conversion. This new method uses a two-stage reaction to minimise equipment size. Furthermore, a carbamate condenser is used to recover unconverted ammonium carbamate (NH_2COONH_4), which makes this process even more efficient.

As the Haber-Bosch process is the standard for industrial scale ammonia synthesis, a novel method was investigated powered by photovoltaics. The method consists of nitrogen passing through a humidifier where water vapor is fed into the electrochemical cell, ammonia is formed on the cathode. The parameters were 0.8 MPa and $20°C$ [15]. Due to significant energy requirements and scalability factors, Haber-Bosch was favoured, given the lower energy consumption varying from 0.58 to 0.81 MJ/mol NH_3.

Conversely, Chemical Looping Ammonia Synthesis (CLAS) offers a more moderate approach by splitting the reaction into steps, allowing for potential efficiency gains under less extreme conditions [8]. CLAS focuses on separating nitrogen fixation and hydrogenation across different reaction stages, which can optimise thermodynamics and kinetics. It requires suitable nitrogen carriers like Metal Nitrides (MNs) that undergo reversible reactions with nitrogen and hydrogen. These carriers react with hydrogen to form ammonia, and then with nitrogen to regenerate the MNs. The process can be driven by additional energy inputs, such as electricity, light, or microwaves, to achieve reactions that are unfavourable in standard conditions. Advances in this area, including electro-, photo-, and plasma-driven CLAS, show promise for more sustainable ammonia production. However, it is still in the developmental or pilot stages and have not yet been proven at a scale comparable to the Haber-Bosch process. In addition, the cost of transitioning to a new technology includes not just the physical infrastructure but also the market's acceptance of the product from the new process. The Haber-Bosch process benefits from an established market presence and trust in its product's consistency and quality. As such, Haber-Bosch is chosen as the process for ammonia synthesis.

The catalyst plays a pivotal role in improving the process performance, lower the energy demand. Ruthenium (Ru)-based catalysts are typically more expensive than the industry standard Fe-KM1. However, cost-benefit analysis of the patented Ru/C catalyst compared to Fe-KM1 reveals that is a worthwhile investment.

Ru/C catalysts offer improved single pass conversions and yield compared to ammonia as the Fe-KM1 catalysts, however at significantly lower pressures (100-120 bar with Ru/C vs 150–250 bar with Fe, with comparable temperatures). Mechanistically this is partially due to the fact that Fe catalysts are inhibited by ammonia, severely capping its maximum achievable conversion, whereas Ru/C catalysts are inhibited by hydrogen and methane, the former of which can be ameliorated through imposing under-stoichiometric reaction conditions and the latter of which may be reduced by ensuring temperatures do not exceed 500°C, through integrating interstage cooling [9]. Specifically, conventional Haber-Bosch in the current day requires approximately 7.78 kWh/kg of NH_3. The proposed process requires only 2.35 kW/kg of NH_3 [10]. Longevity of Ru-based catalysts due to less severe operating conditions inducing less catalyst damage can offset the initial higher investment through reduced catalyst replacement frequency and lower degradation rates.

2.3. Key Performance Indicators (KPIs)

To achieve objective performance evaluation and mitigate decision-making biases within the urea plant design process, the implementation of Key Performance Indicators (KPIs) is essential. Furthermore, KPIs serve as a crucial tool to prioritise efforts by directing resources towards parameters with the most significant impact on operational performance and strategic objectives.

A weighting factor is incorporated into the KPI framework, derived from a pairwise comparison matrix and subsequently normalised. The weighting scheme for both primary and secondary criteria is presented in detail within the supplementary documents and summarised in Figure 2.

MCDA			
	Weighting factor		**Weighting factor**
Economics	**0.23**	Capital Expenditure (CAPEX)	0.50
		Operating Expenditure (OPEX)	0.50
CO2 mitigation and Renewables utilisation	**0.41**	CO2 Emission Intensity	0.33
		Avoided CO2 Emissions	0.26
		Renewable Energy Utilisation	0.41
Thermodynamics	**0.36**	N2 Conversion Rate	0.38
		CO2 Conversion Rate	0.15
		Energy consumption per ton of urea	0.47

Figure 2: Multi Criteria Decision Analysis (MCDA) Weighting Summary

As indicated in Figure 2, prioritisation is accorded to environmental-related and thermodynamic considerations over economic factors. This prioritisation aligns with the project's objective of executing a process design that utilises CO_2 and renewable energy sources, eliminating reliance on fossil fuels. The process is further designed to contribute to the energy transition goals outlined in the Paris Agreement and mitigation of CO_2 emissions. Consequently, the weighting factors for the primary criteria, namely Economics, CO_2 mitigation and Renewable utilisation, and Thermodynamics, are established as 0.23, 0.41, and 0.36, respectively.

This study will subsequently employ a comparative KPI analysis to assess the proposed urea production process against a conventional process, specifically, an existing urea plant. The conventional process utilises Steam Methane Reforming (SMR) for hydrogen and nitrogen production, with natural gas as the feedstock, and does not incorporate renewable energy sources. The conventional process also employs the unmodified Haber-Bosch process for ammonia synthesis. In addition, for urea production, it utilises CO_2 from the combustion of carbon, which does not satisfy the GHG emission mitigation.

3. Renewable-Based Sustainable Materials

3.1. Seawater Reverse Osmosis- Proton Exchange Membrane Electrolysis (SWRO-PEM)

The use of freshwater as a feedstock for the large scale production of hydrogen is likely to disproportionately aggravate competition for freshwater, a resource that is susceptible to shortages. As such, in pursuit of a sustainable future that ensures food and water security for all, technological advancements must be made to leverage abundant resources such as seawater for large-scale hydrogen production. Direct seawater electrolysis shows real promise as pre-processing steps are minimised; however, system lifespan and efficacy are reduced due to impurity buildup, chlorine production, and corrosion of components. For example, recent investigations into novel electrode formulations such as CoOx carbon fibre electrodes found that significant current attenuation (approx. 47%) occurred in alkalinised sea water, and current density degraded to zero after just 50h. Investigations involving the implementation of hard Lewis Acids on electrodes to promote local alkalinity which resists chlorine production and minimises corrosion, have been done, however, current data is only at lab scale, and availability of specialised electrodes significantly reduces the feasibility of such novel mechanisms at this point [11].

Comparatively, coupling industrially mature processes such as Reverse Osmosis and Proton Exchange Membrane Electrolysis to desalinate seawater and generate Hydrogen respectively, is much more feasible.

Comprehensive cost evaluations of the Seawater Reverse Osmosis-Proton Exchange Membrane (SWRO-PEM) process indicate that pre-treatment via Reverse Osmosis (RO) contributes minimally to the total energy requirement, representing merely 0.1%. The production of 1 kg of hydrogen necessitates the desalination of 10 kg of seawater, consuming 55.44 kWh of energy, of which a mere 0.03 kWh is allocated to the RO desalination step. Predominantly, the Proton Exchange Membrane (PEM) electrolysis process accounts for approximately 95% of both the energy demand and operational expenses. Consequently, to reduce environmental impact and optimise the use of renewable energy sources, the RO segment's energy requirements could be effectively met by integrating photovoltaic solar panels onsite. Operational expenditures for RO facilities are primarily comprised of electricity usage, membrane renewal, management of waste streams, chemical supplies, labor, and maintenance and operations (M&O) costs.

However, it should be noted that the above cost analysis is valid for much smaller production capacities (50 tons of hydrogen per day). The economic analysis of the proposed plant, which has significantly higher capacity of 381 tons of hyrogen per day revealed that RO accounts for 14.62% of the coupled process's cost. As such, it is determined that the investment of RO is a feasible solution to permit the usage of the essentially infinite, renewable feedstock of seawater, which will save approx. USD 1,140,095 per year in treated water costs (assuming USD 0.001 per kg of fresh water) [12].

The levelised cost of hydrogen production is approximately USD 3.81 per kg, not accounting for the expenses (SWRO). The inclusion of SWRO water costs results in a marginal increase to about USD 4.85 per kg, as calculated by the PEM model incorporated on Python (discussed in Section 6). The analysis reveals that the addition of SWRO to hydrogen production imposes a minor financial impact on the total cost of hydrogen, due to the relatively minimal energy consumption, capital investments (CAPEX), and operational costs (OPEX) associated with SWRO in comparison to the proton exchange membrane (PEM) electrolysis process.

Furthermore, the energy demands are dominated by PEM electrolysis, which requires 55.44 kWh per kg of hydrogen, whereas SWRO requires only 0.03 kWh to treat the corresponding volume of water. As such the investments into the solar and wind infrastructure's capacity is dominated by the demands of PEM electrolysis.

Research suggests that for viable large scale green hydrogen production, the carbon intensity of electricity generation of the given country must be <0.18 CO_{2-eq} per kWh. While Italy falls short of this goal currently, in line with the current European average of approximately 0.252 kg CO_{2-eq} per kWh. However, the projections by the European Union show that the European average will fall dramatically by 2030 to an indicative high of 0.118 kg CO_{2-eq} per kWh and an indicative low of 0.110 kg CO_{2-eq} per kWh [13]. As such the evidence suggests that within the next decade, Italy will be a viable candidate for large scale green hydrogen production using a SWRO-PEM plant

3.2. Pressure Swing Adsorption (PSA)

Due to the process requiring 1,550 tonnes/day of nitrogen, the following nitrogen purification technology diagram was evaluated to determine which technology is well suited for this process [14]. The diagram is presented in Figure 3.

The PSA was chosen because it provides a low-cost, high reliable feedstock for large-volume users and is commonly used in the gas industries [15]. The PSA mechanism works with the adsorption of air whereas nitrogen is preferentially adsorbed while the oxygen passes through. The nitrogen will be extracted via depressurisation of the vessel allowing the nitrogen to be released from the adsorbent [16].

The rationale behind selecting PSA lies in its operational suitability at a nearly ambient temperature, unlike other methods such as cryogenic distillation, which requires significant energy for cooling. Although, the cryogenic distillation usually offers more purity, modern PSA has demonstrated commercially to achieve high purity of up to 99.9% which is sufficient for many industrial applications such as urea production [17].

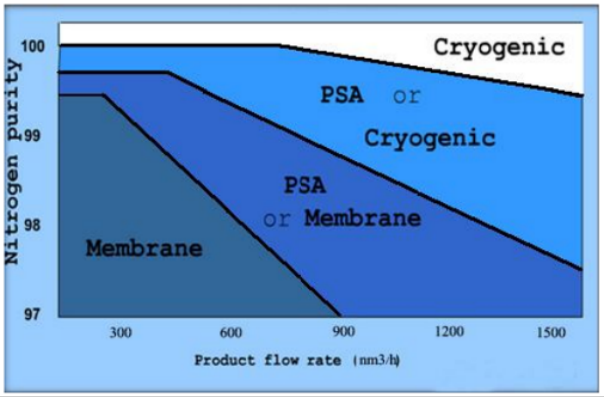

Figure 3: Nitrogen purification technology diagram

The cyclic operation of two distinct adsorption vessels ensures a continuous flow of nitrogen, with one vessel engaged in nitrogen production while the other undergoes depressurisation to expel adsorbed oxygen, consequently vented into the atmosphere. In comparison, membrane separation, founded upon the principle of selective gas permeation, represents an alternative mechanism for nitrogen extraction. This process employs multiple membrane modules, each comprising numerous hollow-fibers, through which gas molecules permeate differentially based on their inherent permeation rates, contingent upon solubility, diffusivity, and desorption characteristics within the hollow-fiber membrane structure. The schematic of a typical PSA system is as shown in Figure 4.

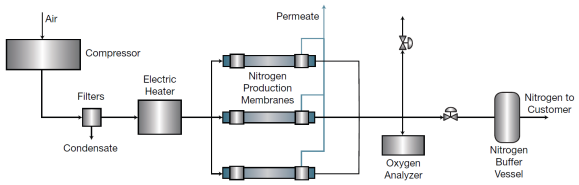

Figure 4: PSA Configuration [15]

The optimisation of nitrogen production via PSA entails a systematic enhancement poised to elevate output from a modest level below 5,000 Standard Cubic Feet per Hour (SCFH) to a notably superior range exceeding 60,000 SCFH, all while maintaining purity levels spanning from 95% to 99.999%. This refinement hinges upon the sequential refinement of the PSA process, wherein compressed air is purified before undergoing selective adsorption by carbon molecular sieves (CMS), packed into an adsorption bed, which primarily targets impurities such as CO_2 and residual moisture [15].

3.3. CO_2 Sources

3.3.1. Direct Air Capture (DAC)

Direct Air capture is one of only a handful of available technologies which allows the direct reduction of CO_2 content in the atmosphere. Carbon Direct Removal (CDR) technologies

are critical modalities which must be integrated into large scale industrial processes alongside the systematic effort of reducing GHG emissions, as CO_2 concentration in the atmosphere is a major contributor to global temperature rise and its associated climate effects.

The proposed DAC process is adopted from the America Physical Society (APS) [18]. This design employs an apparatus known as an "air contactor," through which ambient air passes and interacts with a chemical sorbent i.e. NaOH. This sorbent selectively captures CO_2, which is subsequently released in a concentrated form, Na_2CO_3, which then undergoes Chemical Swing Adsorption (CSA) with $Ca(OH)_2$ in a precipitator for the formation of solid $CaCO_3$, which regenerates the sorbent to be recycled to the air contactor. The precipitant is sent to the Calciner, where thermal decomposition at approximately 900°C [19] fueled by biomethane combustion in the presence of pure O_2 (minimises the formation of NO_x and the dilution of CO_2) releases pure CO_2 and CaO, the latter of which is then sent to a slaker for the regeneration of $Ca(OH)_2$. Pure O_2 is supplied from PSA, discussed in Section 3.2. The pure CO_2 stream is diverted to the urea production process.

Alternative measures for CDR include Bioenergy with Carbon Capture and Storage (BECCS) and reforestation/afforestation. However, DAC offers a unique advantage BECCS and reforestation due to its comparatively lower land requirements, freeing valuable arable land for agriculture and conservation. Estimates suggest that to capture one million tons of CO_2, a DAC plant would need approximately 0.4 km^2 (natural gas powered, with CCS), while forestation would demand 862 km^2 [20].

Furthermore, DAC operates independently of biological growth constraints such as water and nutrient needs, providing a more predictable and rapidly scalable carbon capture solution. Additionally, DAC's operational flexibility allows for deployment in a wide range of environments, including those not conducive to biomass cultivation or reforestation. Moreover, DAC can generate a pure stream of CO_2, beneficial for certain industrial uses and more efficient geological sequestration. The immediacy with which DAC can be implemented, along with its relatively consistent performance, renders it a compelling option in the strategic toolkit for addressing atmospheric CO_2 levels.

3.3.2. Ravenna CCS Facility

The fully operational Ravenna CCS plant is predicted to store upwards of 4 million tonnes of CO_2 by 2027, significantly abating the emissions from a wide range of carbon intensive industries across northern Italy. This presents a reliable stream of highly pure CO_2 at what can be assumed to be a low cost (assumed to be USD 0.04 per kg). This is because the desorption of CO_2 from its underground storage is not an energy intensive process. As such, CO_2 from this CCS facility will compose a large proportion (90%) of the CO_2 required for the urea plant [21].

3.4. Renewable Energy Sources

3.4.1. Solar PV

Italy has made substantial progress in incorporating renewable energy sources within its electricity sector, with a particular emphasis on solar photovoltaic (PV) technology. As of 2021, solar energy accounted for approximately 21.5% of Italy's total renewable electricity production, contributing 25 TWh. This is part of a broader national strategy, as outlined in Italy's National Energy and Climate Plan (NECP), which projects a total installation of around 131 GW of renewable plants by 2030, including approximately 80 GW from solar PV alone. For calculating the solar PV potential to power the urea plants, solar irradiance data is crucial. It provides insights into the amount of solar energy available at a given location, which is key for modeling solar PV output. Solar irradiance data as of 2020 suggests highly consistent irradiance in the Ravenna area rendering the construction of solar panels for a reliable source of energy feasible [19].

3.4.2. Wind

Shallow water offshore wind fans will be constructed and will generate the majority of the electricity generated for the proposed plants. This renewable energy source significantly diminishes greenhouse gas emissions, offering a reliable and scalable power solution that mitigates land use conflicts. The geographical advantage of consistent wind speeds enhances energy generation efficiency, ensuring stable energy supply. Importantly, it offers long-term cost benefits and supports sustainable hydrogen production for urea feedstock. In essence, shallow water offshore wind farms present a compact yet comprehensive solution, promoting environmental stewardship and economic resilience in urea production.

4. Location of the Proposed Plant

Given the necessity for proximity to the Ravenna CCS Facility, Ravenna is chosen as a feasible region for the proposed urea plant. Furthermore, the proximity of the plant to the shore permits the integration of the proposed shallow-water wind farms and Reverse Osmosis-Proton Exchange Membrane Electrolysis plan for hydrogen production. The proposed area is calculated to be around 200,000 m^2, with the proposed plot of land shown below in Figure 5. The solar PV facility will be mounted within this designated area, while the wind turbines will be installed offshore. As depicted in Figure 5, the Ravenna CCS Hub is conveniently located 4.31 km from the proposed site, minimising infrastructure development and transportation costs associated with the CO_2 raw material.

5. Process Description

The block flow diagram in Figure 6 depicts the overall process of the proposed plant which will start with the production of all the raw materials that have been explained in the previous section, which were the SWRO-PEM, PSA, and DAC & Ravenna source for the production of hydrogen, nitrogen, and

Figure 5: Proposed Urea Plant Location

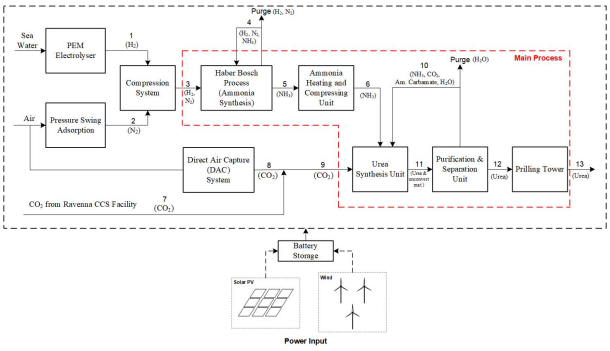

Figure 6: Block Flow Diagram of Ammonia-Urea Plant

CO_2 respectively. In this section, the details of the main process which includes the ammonia synthesis, and the urea synthesis will be explained further.

5.1. Ammonia Synthesis

For the ammonia (NH_3) synthesis, given a feed flow of 1,500 tonnes/day of nitrogen and 380 tonnes/day of hydrogen, a Fixed Bed Reactor (FBR) with 3 reactive beds was selected to accommodate the process. In accordance with Le Chatelier's Principle, lower temperatures and high pressure would shift the reaction forward, however this would limit the rate of reaction. Thus, a combination of high temperature and pressure of 500°C and 100 bar was set as the operating conditions [22], with the help of heterogeneous catalyst (Ru/C) to accommodate lowering the activation energy required for the reaction to take place and increasing the reaction rate, and to ensure the high conversion [9]. Moreover, interstage coolers will be utilised to address the highly exothermic reaction. Therefore, this scheme was chosen to be used in the ammonia synthesis process. Equation 1 shows the ammonia synthesis reaction.

$$N_2(g) + 3H_2(g) \rightleftharpoons 2NH_3(g) \tag{1}$$

Figure 7 shows the Process Flow Diagram (PFD) of ammonia synthesis plant. This PFD flowsheet is simulated in Aspen HYSYS which will be discussed further in the subsequent Section 6.

5.2. Urea Synthesis

In the urea synthesis, Reaction 2 is fast and strongly exothermic, and runs practically to completion if the reaction heat is

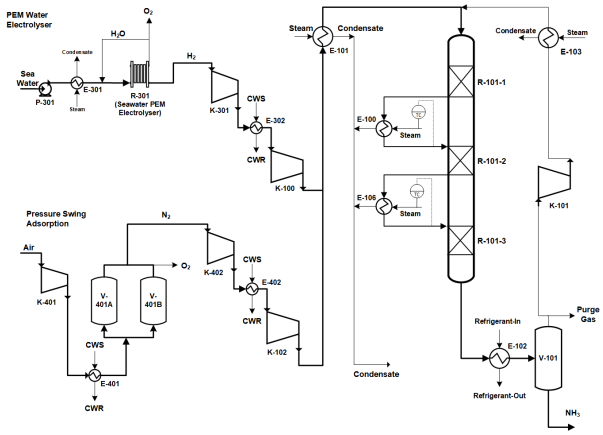

Figure 7: Ammonia PFD

removed, according to Le Chatelier's principle, and the pressure is high enough to force the NH_3 and CO_2 into the liquid phase. Reaction 3 however, is slow and slightly endothermic, so high temperature is required. Since both reactions run in liquid phase and the melting point of ammonium carbamate (AMC) is 153°C, a high temperature is needed. NH_3 and CO_2 are forced into the liquid phase by a high pressure. Therefore, the reactor will operate at T= 180°C and P=150 atm. In reaction 2, NH_3 is chosen to be the excess reactant to avoid such unpractical high pressure at the stoichiometric molar ratio $2NH_3$:$1CO_2$. The maximum achievable urea concentration occurs at the azeotropic ratio, which is approximately $3.4NH_3$:$1CO_2$. Thus, it is determined that the feed mole ratio of NH_3/CO_2 is 3.4. The excess of NH_3 can also reduce the biuret formation, forcing reaction 4 to the urea side [23].

$$2NH_3(g) + CO_2(g) \rightleftharpoons NH_2COONH_4(s) \tag{2}$$

$$NH_2COONH_4(s) \rightleftharpoons H_2O(l) + NH_2CONH_2(s) \tag{3}$$

$$2NH_2CONH_2(s) \rightleftharpoons C_2H_5N_3O_2(s) + NH_3(g) \tag{4}$$

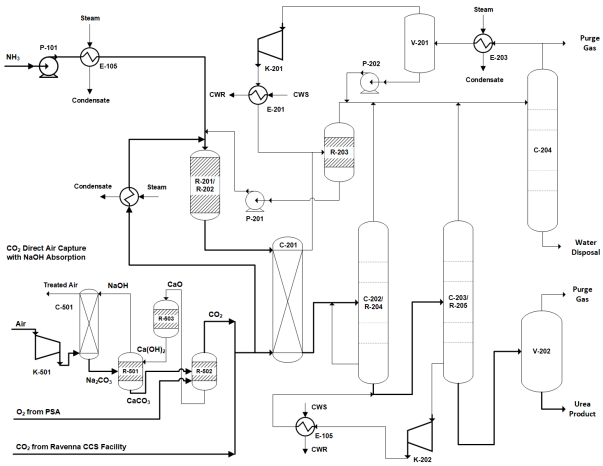

Figure 8: Urea PFD

The Process Flow Diagram, as depicted in Figure 8, is simulated in Aspen HYSYS V11.

6. Simulation

6.1. PEM Electrolysis Model

Equation 1 to 4 shows the mathematical model of PEM electrolyser and also the economic calculation.

$$I_C = \frac{\dot{N}_{H_2} \times 2 \times F}{\eta_F} \tag{5}$$

$$I_A = \frac{I_C}{24 \times 3600} \tag{6}$$

$$C_{\text{total}} = C_{\text{capital}} + C_{\text{operating}} + C_{\text{electricity}} \tag{7}$$

$$LCOH = \frac{C_{\text{total}}}{\dot{N}_{H_2}} \tag{8}$$

I_C represents the current required for the electrolysis process in amperes (A). $\dot{N}_{H_2}$ is the molar flow rate of hydrogen production, measured in moles per second (mol/s). F stands for Faraday's constant, approximately 96,485 C/mol. η_F is the Faraday efficiency, a dimensionless ratio that accounts for the efficiency of the electrolysis process in converting electrical energy into chemical energy stored in hydrogen. I_A calculates the average current over a day, given in amperes (A). The total lifetime cost (C_{total}) associated with the hydrogen production system includes all capital expenditures (C_{capital}) such as the cost of equipment and installation, operating costs ($C_{\text{operating}}$) covering maintenance and labor, and the costs incurred from the electricity ($C_{\text{electricity}}$) consumed during operation, all measured in currency units (e.g., dollars).

The designed code conducts an economic and technical evaluation of a PEM electrolysis system for hydrogen production, targeting a daily output of 381 tonnes. It calculates necessary operational metrics such as the total daily charge and average current required, based on inputs like energy needs per kg of hydrogen, the molar mass of hydrogen, and the system's efficiency. Key assumptions include process efficiency metrics and operational parameters like cell voltage and area, which inform the optimal number of cells needed. The economic analysis encompasses capital and operating costs, informed by the number of cells and an assumption that operating expenses constitute a percentage of capital costs, along with the total electricity cost across the project's lifespan. These calculations yield the Levelised Cost of Hydrogen (LCOH), summarising the project's economic feasibility. Results are visually presented, showcasing the system's viability for large-scale hydrogen production under specified conditions. The methodology underscores a structured approach to evaluating PEM electrolysis for hydrogen production, reflecting assumptions on both the technical and economic fronts.

However, the major drawback of the code is evident in the energy demand, which is calculated, which is unreasonably high. This is partially due to the novelty of PEM electrolysis, which necessitates further innovation to be feasible at the proposed scale, and the semi-empirical nature of the model. As such, the energy used for PEM in the economic analysis is based upon literature sources. As previously mentioned in Section 3, the LCOH of hydrogen using PEM was calculated to be USD 4.85.

6.2. Pressure Swing Adsorption (PSA) Model

The PSA is simply modelled using a component splitter in Aspen HYSYS, which not only facilitates the process itself, but also includes the utilities needed. This approach provides a more rigorous and comprehensive analysis of the energy requirements and costs.

The incoming ambient air of 30°C is compressed into a pressure of 7 bar and will be sent into the main process [24]. The process would produce a nitrogen-rich stream consisting of 98% purity which then will be sent to the main process. The modelling of PSA in Aspen HYSYS is shown in Figure 9.

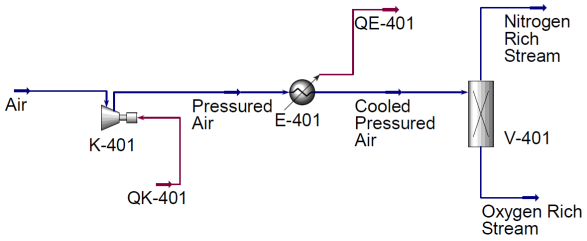

Figure 9: PSA Simulation

6.3. Direct Air Capture (DAC) Model

A DAC modelling is constructed to accommodate power utilised for the fan to convey the atmospheric air. The power fan (P_{fan}) equation [18] is described by Equation 9 - 10.

$$P_{\text{fan}} = \frac{BS\,H_{\text{OG,r}}}{r}\left(\frac{w_G}{w_{\text{Gr}}} \cdot \frac{w_{\text{Lr}}}{w_L}\right)^{0.16} \times \left(k_1 w_G + k_2 w_G^2 + k_3 w_L \exp(k_4 w_G)\right) \ln\left(\frac{1}{1-r}\right) \tag{9}$$

$$H_{OG,r} = \frac{w_{G,r}}{(k_G a_r)} \tag{10}$$

Where B is the design specification of absorber column (m/s), w_G is the velocity through the absorber (m/s) and $w_{G,r}$ is a reference value (m/s), a_r is a reference effective spesific surface, S is the cross-section area (m^2), $H_{OG,r}$ is the height of transfer unit (m), k_G is the gas-phase mass transfer coefficient (m/s), r is the CO_2 capture fraction, w_L is the solution velocity (m/h) and $w_{L,r}$ is a reference value (m/h), k_1 - k_4 is packing parameters.

From the stated values and recommended number in [18] and modelled in Python, it is obtained the power required for the DAC fans is 11.94 MW.

6.4. Haber-Bosch (Ammonia Synthesis) Simulation

In practice, Haber-Bosch integrates intercooling systems to reduce the temperature of processed gases before each stage. To achieve the same outcome in Aspen HYSYS, the process was designed to have three reactors and two coolers. The reaction and kinetics follow the Langmuir-Hinshelwood-Hougen-Watson (LHHW) kinetics model, thus simulating a heterogenous catalytic reaction inside a plug flow reactor [9] . As Aspen HYSYS does not have an FBR, the sequential PFRs are a

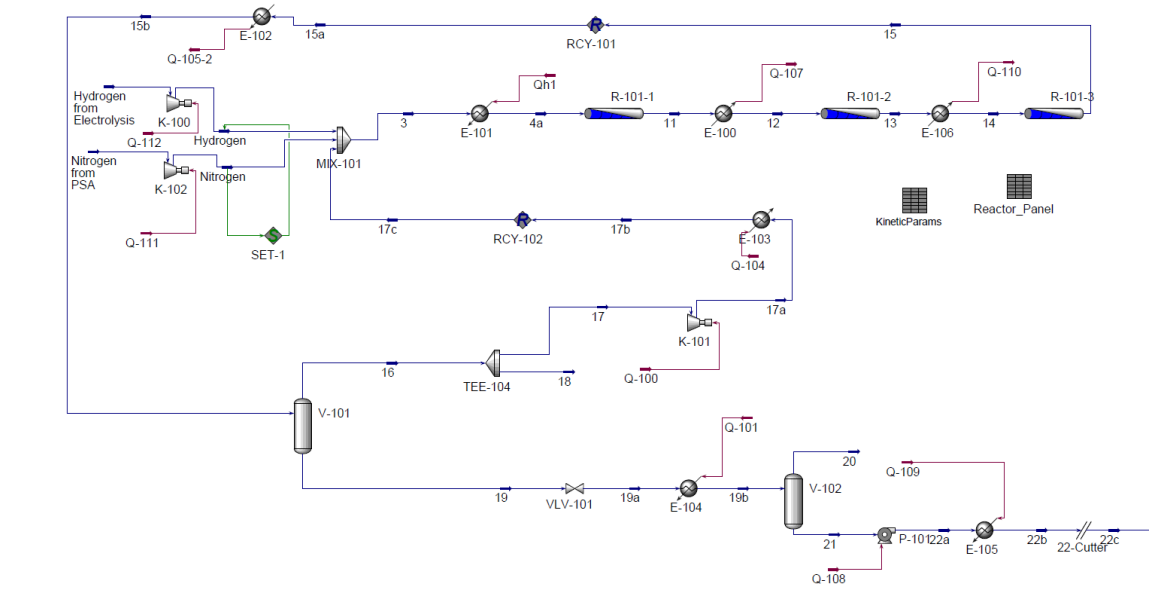

(a)

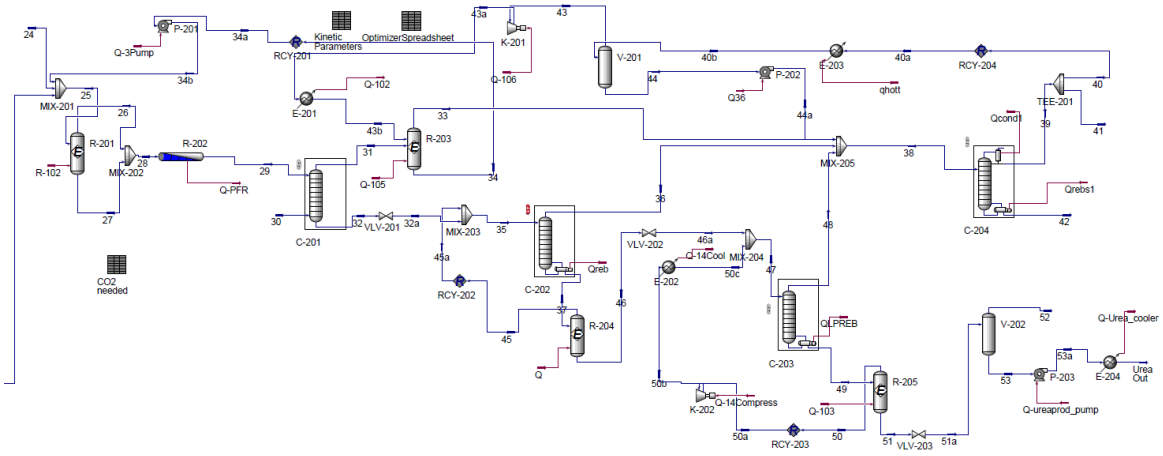

(b)

Figure 10: Aspen HYSYS Flowsheet for (a) Ammonia Plant (b) Urea Plant

proxy of each bed in the reactor with integrated catalyst. The sizing of each PFR in Aspen HYSYS is derived from literature, however, only the sizes of the reacting beds are used. This is due to the previously mentioned limitations of Aspen HYSYS, but also taking account of the assumption that this will have a negligible effect on the accuracy of the final simulation, as only the reacing surfaces are critical.

The Thermodynamic Models Haber-Bosch/Ammonia Production is modelled using the Peng-Robinson Equation of state, give its suitability for modelling non-deal behaving gases under high temperature and pressure as required in the Haber-Bosch. The simulation will also include a recycle stream to further improve the conversion of N_2 and H_2. The reaction kinetics are presented in Table 1 [9]. The inputs for the simulation are shown in Table 2.

With the inputs given, a conversion of 95.3% of nitrogen to ammonia was obtained.

Table 1: Kinetic Parameters for Reaction 1

Reaction	E_a	k_0	β	Order		
				N_2	H_2	NH_3
Forward	23	426	0.5	0.375	-0.25	0
Reverse	23	426	0	-1.125	0.75	1.49

Table 2: Inlet Conditions and Flowrates

Parameter	N_2	H_2	Unit
Inlet Pressure	100	100	bar
Inlet Temperature	138	138	°C
Flowrate	2,300	6,900	kmole/day

6.5. Urea Synthesis Simulation

To simulate the urea process, the main reactor as a PFR is assigned with the input parameters in Table 3 along with CO_2 input flowrate.

Table 3: Parameters input for Urea Synthesis Simulation

Parameter	Value	Unit
Inlet Pressure	152	bar
Inlet Temperature	180	°C
CO_2 as Reactor Feed	950	kmole/day
CO_2 as Stripper Feed	2,300	kmole/day

The NH_3 and CO_2 will react to produce the urea product in the PFR with the kinetics parameter as shown in Table 4. The reaction for AMC formation and decomposition is simulated in the equilibrium reactor, as well as the biuret formation. The reaction rate for the urea process can be seen in Equation 11 and 12:

$$r_{R3} = k_3 \left(C_{H_2NCOO^-} - \frac{C_{H_2O} C_{H_2NCOO^-}}{K_{r4} C_{NH_4^+}} \right) \tag{11}$$

$$r_{R4} = k_4 \left(C_{urea,0} - C_{urea} \right)^2 \tag{12}$$

Table 4: Kinetic Parameters for Urea Reactions

Parameter	**Forward Reaction**	**Reverse Reaction**
A	2.5×10^8	9.6413×10^7
E (J/mol)	23,901	23,901

From the urea reactor, the product flows to the separation units simulated with a stripper column and distillation columns. Three distillation units are assigned to accommodate HP Decomposer, LP Decomposer, and Water Removal Column. This separation section is assigned to increase urea purity and recover unreacted materials, as well as decomposed AMC back to NH_3 and CO_2.

The urea production process simulation employed the UNIQUAC fluid package, chosen for its adeptness with polar components and its established utility in modelling phase equilibria across significant temperature and pressure variations [25].

From the Aspen HYSYS simulation, the proposed plant can produce up to 1,300 tonne/day with 99%-mole and a conversion of Urea reaction of 60.8%. This result meets the required amount of Urea stated in the aforementioned section.

7. Optimisation

7.1. Heat Exchanger Network (HEN)

The approaches used in HEN can be divided into the following: pinch methods and automated methods.

Pinch Analysis Method. Pinch analysis was used to generate the HEN configuration with several key assumptions:

- Constant stream flow rate, heat transfer coefficients and thermodynamic properties
- Utilities are used only to target the final stream
- ΔT_{min} assumed to be 20°C
- C_p of a stream is the same throughout one stream (including input and output)

The assumptions were made to simplify the calculation to focus on the heat transfer aspect without having to account for the variations in the flowrate over time because the simulation is based on a steady state model. As for the choices of ΔT_{min}, a common approach of 20°C is used with the consideration that the amount shall be large enough to ensure an efficient heat transfer but also small enough to be achievable in most industrial processes without excessive energy consumption or equipment cost with the relation of the cross-sectional area of the heat exchanger [26].

The following thermodynamic rules must be followed to ensure feasible heat transfer:

- Below the pinch : $\mathrm{FCp}_H \geq F\mathrm{Cp}_C$
- Above the pinch : $\mathrm{FCp}_C \geq F\mathrm{Cp}_H$

The pinch point is identified, which is the narrowest gap between the hot and cold composite curves, indicating the most critical area of heat recovery in the process. The pinch point was found to be at T=67.49°C. Since the ΔT_{min} was set to be 20°C, the pinch for the region above and below the pinch are 77.49 °C and 57.49 °C, respectively.

HEN Superstructure. The stream matching is conducted according to the aforementioned assumptions and rules. The resulting superstructure can be seen in Figure 11 below.

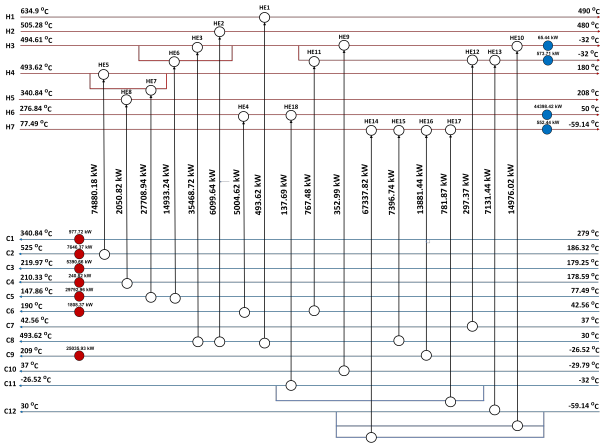

Figure 11: HEN structure

After conducting the stream exchange, the result of the HEN superstructure suggests that the amount of cooling utility required is 45,590.01 kW, while the amount of hot utility required

is 70,892.82 kW that would result in the reduction of the utilities required by 86%.

Utility Cost Minimisation (General algebraic modeling system, GAMS) Automated Method. To corroborate the findings from the problem table, find the minimum cost of utilities used, and optimise the minimum utility costs, the streams were inputted into GAMS optimiser. Equation 13 displays the objective function to be minimised by GAMS via linear programming (LP):

$$\begin{aligned}\min \text{COST} = (&Q_{\text{HF}} \cdot C_i + Q_{\text{HP}} \cdot C_i + Q_{\text{LP}} \cdot C_i \\ &+ Q_w \cdot C_i + Q_{\text{ref2}} \cdot C_i) \times 60\,\text{s}^{-1} \\ &\times 60\,\text{min}^{-1} \times 8,000\,\text{hr yr}^{-1}\end{aligned} \tag{13}$$

The chosen utilities are based on the common utilities being used in a process plant which are fuels, high pressure stream, low pressure steam, and refrigerants. The specific refrigerant in this case consists of a mixture of ethane and propane which has a cooling temperature of -40°C. This choice aligns with prevalent standards for cooling applications within such facilities. Additionally, it is assumed that the plant operates for 8,000 hours a year.

From the analysis conducted by GAMS, it has been determined that the minimum required utilities only consist of a low-pressure steam which is 78,217.7 kJ, reducing the required utility by 90.6%.

Although the reduction in utility differs between the superstructure and the automated method. The superstructure approach is preferred as it considers the pinch analysis alongside the thermodynamic rule which makes it more thorough.

7.2. Renewable Energy Optimisation

The optimisation procedure was executed utilising the Pyomo optimisation framework. Mixed-Integer Non-Linear Programming (MINLP) is used as the described problem necessitates a solver which can handle discrete decisions and non-linear dynamics, including the division-based non-linearity in ratio optimisation, ensuring solutions are both accurate and economically viable. Gurobi was selected as the solver of choice due to its robustness in handling MINLP problems and its computational efficiency due to its high-level pre-processing and heuristic framework.

- Variables: The size of solar and wind installations, generation output, surplus generation (spill) and self- consumption.
- Constraints:
  1. Generation Capacities: Each solar panel and wind turbine can only produce a certain amount of electricity, limiting the maximum generation.
  2. Load Demand Fulfillment: The total electricity generated must be enough to meet the demand from consumers or the grid at all times.
  3. Renewable generation spill limitations: The model seeks to minimise waste by limiting how much generated power goes unused.
- Objective Function: Minimising the total cost of generation, including costs associated with solar and wind generation and penalties for unmet demand or excessive spill.

Minimise Cost:

$$\sum 45 \frac{\text{USD}}{\text{MW}} \times (W_{\text{PV}}) + \sum 53 \frac{\text{USD}}{\text{MW}} \times (W_{\text{wnd}})$$

The generation of electricity via wind power, denoted as W_{wnd}, is contingent upon variables such as wind speed V_{wn}, air density ρ_a, the turbine's swept area A_{wt}, the power coefficient C_p, the efficiency of the generator η_{gen}, the efficiency of the wind turbine η_{wn}, and the total number of turbines employed N_{wt}. This relationship is outlined in Equation 15 - 16.

$$Q = I_b \times A_{PV} \tag{14}$$

$$W_{PV} = \eta_{PV} \times Q \tag{15}$$

$$W_{\text{wnd}} = \frac{1}{2} \rho_a A_{\text{wt}} V_{\text{wn}}^3 C_p N_{\text{wt}} \eta_{\text{wn}} \eta_{\text{gen}} \tag{16}$$

The optimisation algorithm's procedural architecture and resultant outcomes are visually delineated in Figure 12.

Algorithm 1 Energy Gen. and Storage Opt. Algorithm

Input: Solar Irradiance and Wind Speed data for Italy.
Params: η_{PV}, A_{PV}, ρ, A_{wt}, C_p, η_g, N_{wt}, B_{max}, η_{ch}, η_{dis}, $Cost_{kWh}$
Init: $iter \leftarrow 0$, $SoC \leftarrow B_{max}/2$
$Load \leftarrow$ Urea + PEM + PSA + DAC load
while $iter < max.iteration$ **do**
  $Solar_{out} \leftarrow U_{solar}(I(t), \eta_{PV}, A_{PV})$
  $Wind_{out} \leftarrow U_{wind}(V(t), \rho, A_{wt}, C_p, \eta_g)$
  $Gen_{tot} \leftarrow S_{out} + W_{out}$
  $Batt_{charge} \leftarrow U_{charge}(Gen_{tot}, Load, SoC, \eta_{ch})$
  $Batt_{discharge} \leftarrow U_{discharge}(Gen_{tot}, Load, SoC, \eta_{dis})$
  State of Charge $(SoC) \leftarrow SoC + B_{ch} \cdot \eta_{ch} - B_{dis}/\eta_{dis}$
  Ensure $0 \leq SoC \leq B_{max}$
  $Gen_{tot} \leftarrow Gen_{tot} + B_{dis} - B_{ch}$
  Ensure $Gen_{tot} \geq Load$
  $x \leftarrow [Solar_{out}, Wind_{out}, Batt_{charge}, Batt_{discharge}]$
  $f \leftarrow obj\_func()$
  Minimise$(f + Cost_{kWh} \cdot (B_{ch} + B_{dis}))$
  Use Gurobi solver to optimise the model
  $iter \leftarrow iter + 1$
end while

Figure 12 presents the transient fluctuations of wind and solar PV electricity generation over time for the proposed plant. A

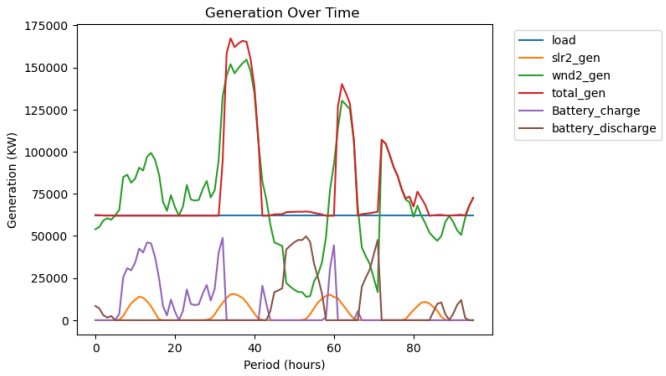

Figure 12: Optimisation Result for Renewable Power Generation

notable challenge associated with these renewable energy technologies is their inherent intermittency, characterised by significant fluctuations in electricity generation over time. To address this, an evaluation of several performance indicators for each technology is incorporated, namely the maximum generation capacity, the average generation capacity, and the capacity factor. Our analysis indicates that the maximal electrical output attainable from solar photovoltaic (PV) systems and wind power plants is 15.6 MW and 154.7 MW, respectively. However, the average electrical generation from solar PV systems and wind power stands at 3.9 MW and 73.7 MW, respectively. Consequently, the capacity factor, defined as the quotient of the average electricity generation and the maximum generation capacity, was determined to be 25% for solar PV systems and 48% for wind power. The required area for solar PV and wind is 89,200 m^2 and 65,906 m^2, respectively. To better improve the performance of the renewable electricity generation, an energy storage is installed in the electricity system. Thus, an excess of electricity will be stored during its peak electricity generation. Based on the optimisation procedure, an energy storage with a capacity of 352 MW must be installed to ensure the power system can meet the load demand at all time.

8. Economic Analysis

The economic assessment indicates a promising fiscal health and viability. It is assumed that the proposed renewable urea plant has a 20-year operational life after a 2-year construction period. The breakdown of the CAPEX, which includes the total module cost, the cost of land, and working capital, amounts to a significant but strategic investment, with working capital being a prudent 15% of the Fixed Capital Investment (FCI). This allocation ensures that the plant has sufficient liquidity to sustain initial operations. The detail of the CAPEX is summarised in Table 5.

The land allocation for the renewable urea plant has been planned to ensure the optimal use of resources and operational efficiency. Spanning a total of 200,000 m^2, the land is apportioned into three primary areas: 50,000 m^2 dedicated to the urea plant itself, where the core production processes will take place; 120,000 m^2 allocated for the solar PV installation, which

Table 5: Capital Expenditure for Urea Plant

Description	Price
Total Module Cost	USD 395,060,000
Cost of Land	USD 60,000,000
Working Capital	USD 41,000,000

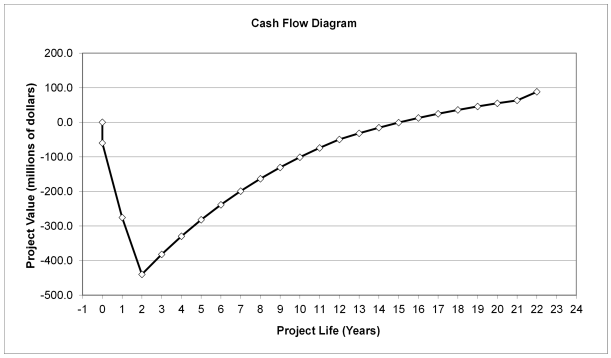

Figure 13: Optimisation Result for Renewable Power Generation

will provide a sustainable and cost-effective power supply; and 30,000 m^2 reserved for wind energy infrastructure, further reinforcing the plant's commitment to renewable energy sources.

Moreover, the OPEX is meticulously categorised into Direct, Fixed, and General Manufacturing Costs, allowing for a nuanced understanding of the ongoing financial demands. This methodical approach aligns with industry best practices and underscores the thoroughness of the financial planning.

Table 6: Basis calculation for Operational Expenditure

Description	Price
Raw material cost (C_{RM})	USD 13,917,713
Cost of Utilities (C_{UT})	USD 60,000,000
Cost of Operating Labor (C_{OL})	USD 936,740

The following equation, as adopted from [27], is used for calculating the OPEX for the urea plant.

$$OPEX = 0.18FCI + 2.73C_{OL} + 1.23(C_{UT} + C_{WT} + C_{RM}) \quad (17)$$

According to the economic calculation, the required OPEX is USD 107,193,325. The Discounted Profitability Criterion accentuates the attractiveness of this venture with a Net Present Value (NPV) of USD 88.17mn, surpassing the threshold typically used to gauge the profitability of chemical plants. The Discounted Payback Period of 8.3 years falls comfortably within the industry standard of 5-10 years, reinforcing the attractiveness of this plant. The Internal Rate of Return (IRR) stands at 12.56%, indicative of a potent return on investment given that rates between 10-20% are deemed profitable.

Furthermore, leveraging the acquisition and sale of carbon credits through the carbon market accommodated by the EU Emissions Trading System (ETS) will result in a shorter pay-

back period of 6.7 years. This is determined through comparative LCA assessments of CO_2 emissions between the conventional urea process and the proposed sustainable urea plant and calculating the revenue based on the product of the sale price of CO_2 from S&P Global (USD 60/ mt CO_{2-eq}) and the avoided emissions.

In conclusion, the renewable urea plant presents a highly attractive proposition for investors. Its financial indicators not only meet the industry's conventional thresholds but also promise a robust return profile. The Cash Flow Diagram, as depicted in Figure 13, convincingly illustrates a progressive financial uptick, reflecting the project's capacity to evolve from initial expenditure to profit generation, affirming its viability as a wise financial endeavor with substantial economic prospects.

9. Environmental Analysis

The sustainable urea production plant has been designed to utilise carbon dioxide emissions, supported with renewable energy and lower energy-intensive processes. This section focuses on the environmental analysis evaluated with the Life Cycle Assessment (LCA) method to review the efficiency and the environmental impact of the proposed process. The evaluation is based on the capacity of the proposed plant, 456 kT/year of urea production. A proportional mass-based allocation is assigned for other materials.

The LCA is obtained from the LCA software simulation, openLCA, to give quantified results on the environmental impact. openLCA allows to evaluation of the cradle-to-gate system boundary resulting in a comprehensive evaluation process. The system boundary of the proposed plant for the LCA is captured in Figure 14. The material input for the LCA is seawater, air, and CO_2 with electrification from green electricity and catalyst for the process. Urea as a main product is set for the output along with CO_2 emissions and wastewater to be treated. This LCA will run aside from the construction, maintenance, and materials transport related to the proposed plant.

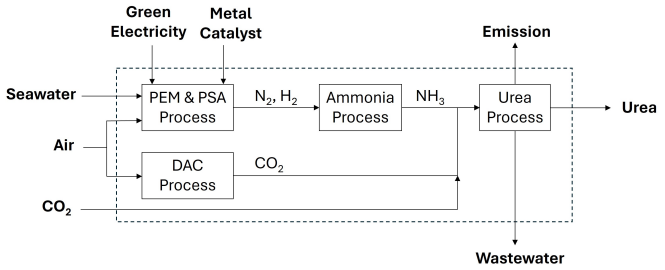

Figure 14: System Boundary for LCA

The "ReCiPe Midpoint (H) 2016 V1.13" is applied for the impact assessment method. This is the most common method principles that take into account 100-year time-framing for climate change (GWP100), ozone depletion, and ionising radiation [28]. This approach provides a wide-ranging and uniform evaluation of the effects on various environmental categories.

In this assessment, five main impacts are observed: Global Warming Potential (GWP), Freshwater Ecotoxicity Potential (FETP), Human Toxicity Potential (HTP), Land Occupation (LO), and Water Consumption (WC). This consideration was because of their general impacts on the environment and the understandability of the public [29]. Other environmental impacts are presented as well to broaden the view of the global effects.

Figure 15 depicts the assessment result carried out with OpenLCA. The figure shows that most of the impact was from the H_2 production process. It is caused by the large seawater flow rate feed to the process inheriting a big amount of environmental impact. Consecutively, catalyst production has the second number environmental impact due to its conventional-made process. It is worth noting that the catalyst process also requires green transitions to support this sustainable Urea process. The N_2 production has a small impact on the environment because of its natural feed introduced to the system and less equipment introduced. The CO_2 production occupies near zero impacts because most of the flows are from the Ravenna CCS Facility.

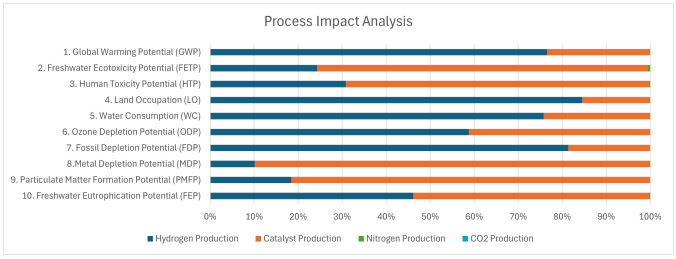

Figure 15: Environmental Impacts on Each Input Process Production

The high GWP and LO impacts on H_2 production are caused by the large amount of seawater required and the number of process steps to generate the hydrogen. While the WC for hydrogen production is utilised to regenerate the RO module when it reaches the saturation condition. A review of water usage in the regeneration process is needed to reduce water consumption. The catalyst process has more impact on HTP and FETP due to the solid process handling that increases the possibility of human and environmental exposure. In addition, the metal material impregnated in the catalyst also has the possibility for toxicity impact. To lower this impact, the development of catalyst materials and production processes is required.

10. KPI Comparative Analysis

A comparative analysis of Key Performance Indicators (KPIs) for two different urea production processes was conducted. As a comparison, a study of conventional urea production plant conducted by Jeenchaya and Siemanonda was used [30].

Based on the KPI criteria along with their decision weights as specified in Section 2.3, a weighted sum approach was employed to evaluate the overall performance of each process. The proposed sustainable urea plant and the conventional urea plant received total scores of 0.291 and 0.854, respectively. In this KPI-based assessment framework, a lower score signifies a

more favourable production process due to its better alignment with the design objectives. A detailed breakdown of the total scores across various categories, including economics, CO_2 mitigation and renewables integration, and thermodynamics, is presented in Figure 16.

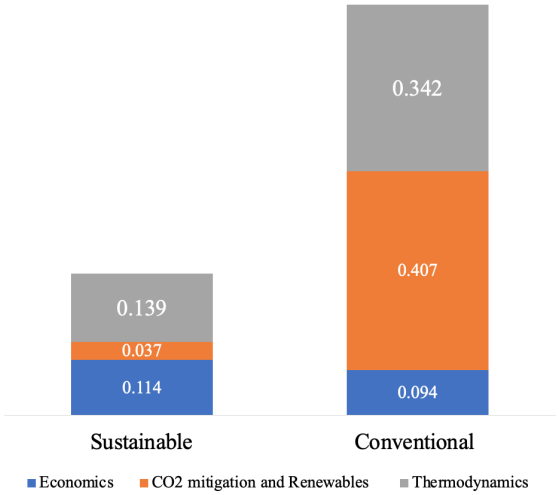

Figure 16: The KPI Result Comparison Between The Conventional Plant and The Proposed Plant

11. Conclusion

This research introduces a novel chemical process utilising CO_2 to produce urea in Italy, powered by renewable energy sources. The process involves a holistic approach, starting from the generation of raw materials: SWRO-PEM electrolysis is used for hydrogen production, PSA technology for nitrogen, and DAC coupled with Ravenna CCS for CO_2 stream. Advanced technologies, including a ruthenium-based catalyst in the Haber-Bosch process, are implemented for urea synthesis. Additionally, this study evaluates the optimal mix of Solar PV and wind power to sustain the energy requirements of the process.

The design capacity of the urea production facility is targeted at 1,300 tonnes per day with a product purity of 99%. A Key Performance Indicator (KPI) framework was established to assess the superiority of this novel process over traditional methods. Two significant optimisations were conducted to enhance the system's efficiency: the first involves heat exchanger integration, employing pinch analysis and an automated method that demonstrated an 86% reduction in utility usage. The second optimisation focused on renewable energy, achieving a maximum output of 15.6 MW from Solar-PV and 154.7 MW amount from wind energy, sufficiently powering the plant.

An economic evaluation reveals that the novel plant is expected to achieve a payback period of 8.3 years, with an internal rate of return of 12.56%. Integration into the EU ETS by selling carbon credits could further reduce the payback period to 6.7 years, underscoring the plant's financial attractiveness and potential high returns for investors.

Furthermore, an environmental assessment identified the SWRO-PEM process as the major contributor to environmental impact. However, comprehensive KPI analysis affirmed that the novel method is more advantageous than conventional urea production techniques. This research demonstrates that innovative approaches to raw material generation and process execution, combined with the integration of renewable energies, offer a promising avenue for significant CO_2 reduction in the future. This strategy not only mitigates environmental impact but also enhances the sustainability and economic viability of urea production.

Acknowledgement

The completion of this paper is deeply indebted to the invaluable guidance and expertise of our esteemed supervisors: Dr. Maria Papathanasiou, Dr. Ronny Pini, and Dr. Andrea Bernardi. Their knowledge and support guided us to reach this final paper. We are also grateful to Muhammad Falakhul Insan for his significant contributions during the initial stages of drafting this paper.

References

[1] EU economy greenhouse gas emissions: -5.3% in q2 2023 - eurostat. URL https://ec.europa.eu/eurostat/web/products-eurostat-news/w/ddn-20231115-1#:~:text=In%20the%20second%20quarter%20of,of%20CO2%2Deq).

[2] EU economy greenhouse gas emissions: -7.1% in q3 2023 - eurostat. URL https://ec.europa.eu/eurostat/web/products-eurostat-news/w/ddn-20240214-1#:~:text=In%20the%20third%20quarter%20of,of%20CO2%2Deq).

[3] H. Ritchie, M. Roser, P. Rosado, Energy. URL https://ourworldindata.org/co2/country/italy

[4] Agriculture - italy | statista market forecast. URL https://www.statista.com/outlook/io/agriculture/italy

[5] V. Kyriakou, I. Garagounis, A. Vourros, E. Vasileiou, M. Stoukides, An electrochemical haber-bosch process 4 (1) 142–158. doi:10.1016/j.joule.2019.10.006. URL https://linkinghub.elsevier.com/retrieve/pii/S2542435119305227

[6] A. Edrisi, Z. Mansoori, B. Dabir, Urea synthesis using chemical looping process – techno-economic evaluation of a novel plant configuration for a green production 44 42–51. doi:10.1016/j.ijggc.2015.10.020. URL https://www.sciencedirect.com/science/article/pii/S1750583615301079

[7] Blog 4: Operational experience with a running ultra-low energy urea plant | stamicarbon. URL https://www.stamicarbon.com/

[8] S. Feng, W. Gao, J. Guo, H. Cao, P. Chen, Electrodriven chemical looping ammonia synthesis mediated by lithium imide 8 (3) 1567–1574. doi:10.1021/acsenergylett.2c02730. URL https://pubs.acs.org/doi/10.1021/acsenergylett.2c02730

[9] A. Tripodi, M. Compagnoni, E. Bahadori, I. Rossetti, Process simulation of ammonia synthesis over optimized ru/c catalyst and multibed fe + ru configurations 66 176–186. doi:10.1016/j.jiec.2018.05.027. URL https://linkinghub.elsevier.com/retrieve/pii/S1226086X18302569

[10] JGC corporation demonstrates "world's first" carbon-free ammonia energy cycle. URL https://ammoniaenergy.org/articles/

[11] J. Guo, Y. Zheng, Z. Hu, C. Zheng, J. Mao, K. Du, M. Jaroniec, S.-Z. Qiao, T. Ling, Direct seawater electrolysis by adjusting the local reaction environment of a catalyst 8 (3) 264–272. doi:10.1038/s41560-023-01195-x.
URL https://www.nature.com/articles/s41560-023-01195-x

[12] M. A. Khan, T. Al-Attas, S. Roy, M. M. Rahman, N. Ghaffour, V. Thangadurai, S. Larter, J. Hu, P. M. Ajayan, M. G. Kibria, Seawater electrolysis for hydrogen production: a solution looking for a problem? 14 (9) 4831–4839. doi:10.1039/D1EE00870F.
URL https://pubs.rsc.org/en/content/articlelanding/2021/ee/d1ee00870f

[13] Greenhouse gas emission intensity of electricity generation — european environment agency.
URL https://www.eea.europa.eu/data-and-maps/daviz/co2-emission-intensity-14/#tab-chart_7

[14] A. s. emrani, M. Saber, F. Farhadi, A decision tree for technology selection of nitrogen production plants 45 (1). doi:10.22059/jchpe.2011.23477.
URL https://doi.org/10.22059/jchpe.2011.23477

[15] Producing nitrogen via pressure swing adsorption.
URL https://www.aiche.org/resources/publications/cep/2012/june/producing-nitrogen-pressure-swing-adsorption

[16] N. Lemcoff, Nitrogen separation from air by pressure swing adsorption, in: Studies in Surface Science and Catalysis, Vol. 120, Elsevier, pp. 347–370. doi:10.1016/S0167-2991(99)80557-6.
URL https://linkinghub.elsevier.com/retrieve/pii/S0167299199805576

[17] Yumpu.com, Pressure swing adsorption plants - linde engineering.
URL https://www.yumpu.com/en/document/view/50726422/pressure-swing-adsorption-plants-linde-engineering

[18] M. Mazzotti, R. Baciocchi, M. J. Desmond, R. H. Socolow, Direct air capture of CO2 with chemicals: optimization of a two-loop hydroxide carbonate system using a countercurrent air-liquid contactor 118 (1) 119–135. doi:10.1007/s10584-012-0679-y.
URL https://doi.org/10.1007/s10584-012-0679-y

[19] M. Mostafa, C. Antonicelli, C. Varela, D. Barletta, E. Zondervan, Capturing CO2 from the atmosphere: Design and analysis of a large-scale DAC facility 4 100060. doi:10.1016/j.ccst.2022.100060.
URL https://www.sciencedirect.com/science/article/pii/S2772656822000318

[20] K. Lebling, H. Leslie-Bole, Z. Byrum, L. Bridgwater, 6 things to know about direct air capture.
URL https://www.wri.org/insights/

[21] D. Meth-Cohn, Ravenna CCS - the CCUS hub.
URL https://ccushub.ogci.com/focus_hubs/ravenna/

[22] A. Sánchez, M. Martín, Optimal renewable production of ammonia from water and air 178 325–342. doi:10.1016/j.jclepro.2017.12.279.
URL https://linkinghub.elsevier.com/retrieve/pii/S0959652617332730

[23] J. Meessen, Urea synthesis 86 (12) 2180–2189. doi:10.1002/cite.201400064.
URL https://onlinelibrary.wiley.com/doi/10.1002/cite.201400064

[24] A. Syakdani, Y. Bow, Rusdianasari, M. Taufik, Analysis of cooler performance in air supply feed for nitrogen production process using pressure swing adsorption (PSA) method 1167 012055. doi:10.1088/1742-6596/1167/1/012055.
URL https://iopscience.iop.org/article/10.1088/1742-6596/1167/1/012055

[25] Y. Dadmohammadi, S. Gebreyohannes, A. M. Abudour, B. J. Neely, K. A. M. Gasem, Representation and prediction of vapor–liquid equilibrium using the peng–robinson equation of state and UNIQUAC activity coefficient model 55 (4) 1088–1101. doi:10.1021/acs.iecr.5b03475.
URL https://pubs.acs.org/doi/10.1021/acs.iecr.5b03475

[26] R. Smith, Chemical process design and integration, Wiley.

[27] Analysis, synthesis, and design of chemical processes.

[28] M. A. J. Huijbregts, Z. J. N. Steinmann, P. M. F. Elshout, G. Stam, F. Verones, M. Vieira, M. Zijp, A. Hollander, R. van Zelm, ReCiPe2016: a harmonised life cycle impact assessment method at midpoint and endpoint level 22 (2) 138–147. doi:10.1007/s11367-016-1246-y.
URL https://doi.org/10.1007/s11367-016-1246-y

[29] S. K. Masjedi, A. Kazemi, M. Moeinnadini, E. Khaki, S. I. Olsen, Urea production: An absolute environmental sustainability assessment 908 168225. doi:10.1016/j.scitotenv.2023.168225.
URL https://www.sciencedirect.com/science/article/pii/S0048969723068523

[30] J. Jeenchay, K. Siemanond, Ammonia/urea production process simulation/optimization with techno-economic analysis, in: A. Friedl, J. J. Klemeš, S. Radl, P. S. Varbanov, T. Wallek (Eds.), Computer Aided Chemical Engineering, Vol. 43 of 28 European Symposium on Computer Aided Process Engineering, Elsevier, pp. 385–390. doi:10.1016/B978-0-444-64235-6.50070-X.
URL https://www.sciencedirect.com/science/article/pii/B978044464235650070X